Supplementary Material

From temporal to spatial topography – Hierarchy of neural dynamics in higher- and lower-order networks shapes their complexity

Mehrshad Golesorkhi[1,2,#], Javier Gomez-Pilar[3,4,#], Yasir Çatal[2], Shankar Tumati[5], Mustapha C. E. Yagoub[6], Emmanuel A. Stamatakis[7], Georg Northoff[2,6,7,*]

1 School of Electrical Engineering and Computer Science, University of Ottawa, Ottawa, Canada
2 Mind, Brain Imaging and Neuroethics Research Unit, Institute of Mental Health, Royal Ottawa Mental Health Centre and University of Ottawa, Ottawa, Canada
3 Biomedical Engineering Group, University of Valladolid, Paseo de Belén, 15, 47011 Valladolid, Spain
4 Centro de Investigación Biomédica en Red en Bioingeniería, Biomateriales y Nanomedicina, (CIBER-BBN), Spain
5 Division of Anaesthesia, School of Clinical Medicine, University of Cambridge, Cambridge, UK
6 Centre for Cognition and Brain Disorders, Hangzhou Normal University, Hangzhou, China
7 Mental Health Centre, Zhejiang University School of Medicine, Hangzhou, Zhejiang, China

# Equal contribution as first authors
* Corresponding author

Supplementary Analyses:

Validation of LZC statistical tests through non-parametric testing

To further validate our previous main results, nonparametric testing was also performed for our resting and task state results. The difference in resting state LZC values among the networks was tested using Kruskal-Wallis non-parametric test which showed significant ($p < 0.001$) differences among the 12 networks ($H = 141.45, \eta^2 = 0.19$). Mann-Whiney test also showed significant ($p < 0.001$) differences between resting state LZC values of lower- ($n = 331, median = 1.05$) and higher-order ($n = 386, median = 0.94$) categories ($U = 83476.50, \eta^2 = 0.07$).

Our task state results were also validated using non-parametric testing. First, lower- and higher-order task data were divided into four combinations of task (MOVIE vs. RET) and category (lower- vs. higher-order) factors. Kruskal-Wallis test showed significant ($p < 0.001$) differences among these four categories ($H = 321.99, \eta^2 = 0.22$). In order to further validate the difference between lower- and higher-order categories, two separate Mann-Whiney tests (one for each task) were performed validating our previous results in both MOVIE ($U = 77071, \eta^2 = 0.03, n_1 = 331, median_1 = 1.05, n_2 = 386, median_2 = 0.94$) and RET ($U = 80296, \eta^2 = 0.05, n_1 = 331, median_1 = 1.10, n_2 = 386, median_2 = 1.04$) with adjusted $p < 0.001$.

The difference among the 12 networks in the two tasks was also validated first by dividing the LZC values into 24 categories (12 networks x 2 tasks) and then performing Kruskal-Wallis test. The non-parametric test revealed significant differences ($p < 0.001$) differences among the categories ($H = 504.59, \eta^2 = 0.34$). In the next step the effect of network alone was investigated with two separate Kruskal-Wallis tests: each one the LZC values of a specific task over all the 12 networks. These two tests also validated our previous results indicating significant ($p < 0.001$) differences of LZC values among the networks in MOVIE ($H = 133.87, \eta^2 = 0.17$) and RET ($H = 144.78, \eta^2 = 0.19$).

Rest to task mediation analysis

To explore whether MF during rest has any effect on the change in LZC from rest to task state, we performed a mediation analysis on the LZC and MF-REST values (Supp. Fig. 7). In the model, the effect of LZC-REST on LZC-MOVIE (LZC-RET) was investigated considering MF-REST as the mediator. This allowed us to explore whether the relationship between LZC during REST and MOVIE (RET) is mediated by MF during REST. The indirect effect was 0.84 * 0.23 = 0.17 (-1.01 * 0.34 = -0.34). We tested the significance of this indirect effect using bootstrapping procedures [1] in the mediation library [2] of R. Unstandardized indirect effects were computed for each of 1000 bootstrapped samples, and the 95% confidence interval was computed by determining the indirect effects at the 2.5th and 97.5th percentiles.

The bootstrapped unstandardized indirect effect was 0.16 (-0.24), and the 95% confidence interval ranged from 0.10 to 0.22 (-0.29 to -0.19). Thus, the indirect effect was statistically significant ($p < 0.001$) showing that MF-REST can indeed be considered as a partial mediator for the change in LZC from rest to task states. It is worth to mention that the mediation analysis was performed with (the above results) and without averaging over subjects to control for the inter-individual effect in bootstrapping. In the with-averaging analysis, first, the data was averaged over subjects then fed into the model, but in the latter one, the subject-level data was used.

In the without-averaging model, the subject-level data was fed into our mediation model. Like before, LZC-REST was used as the independent variable, LZC-MOVIE (LZC-RET) as the dependent one and MF-REST as the mediator. The indirect effect was 0.64 * 0.33 = 0.21 (-0.64 * 0.14 = -0.08). The bootstrapped unstandardized indirect effect was 0.21 (-0.09), and the 95% confidence interval ranged from 0.21 to 0.22 (-0.099 to -0.09). Thus, the indirect effect was statistically significant ($p<0.001$), confirming our original with-averaging results.

Simulations to validate LZC in presence of motion noise in fMRI

To investigate the potential effect of motion on LZC-MF relationship, we simulated 5000 pink noise signals with 900 time points and perturbed 1%, 2%, 5% and 10% of time points selected randomly from a uniform distribution between -4 and 4. In Supp. Fig. 7A, bar plots depict LZC values with and without the perturbation. It can be seen that even with a very high number of time points (10%), the change in LZC is only about 0.05. In Fig. 7B, LZC and MF values before and after each other were plotted. Spearman correlations were performed due to the skewed nature of the measures. As can be seen, the correlation coefficient *r* is practically the same between no motion and different amounts of motion (non-significant differences). These results together show that with effective care to motion artifacts [3,4,5], LZC can be used safely with fMRI data

Supplementary Figures:

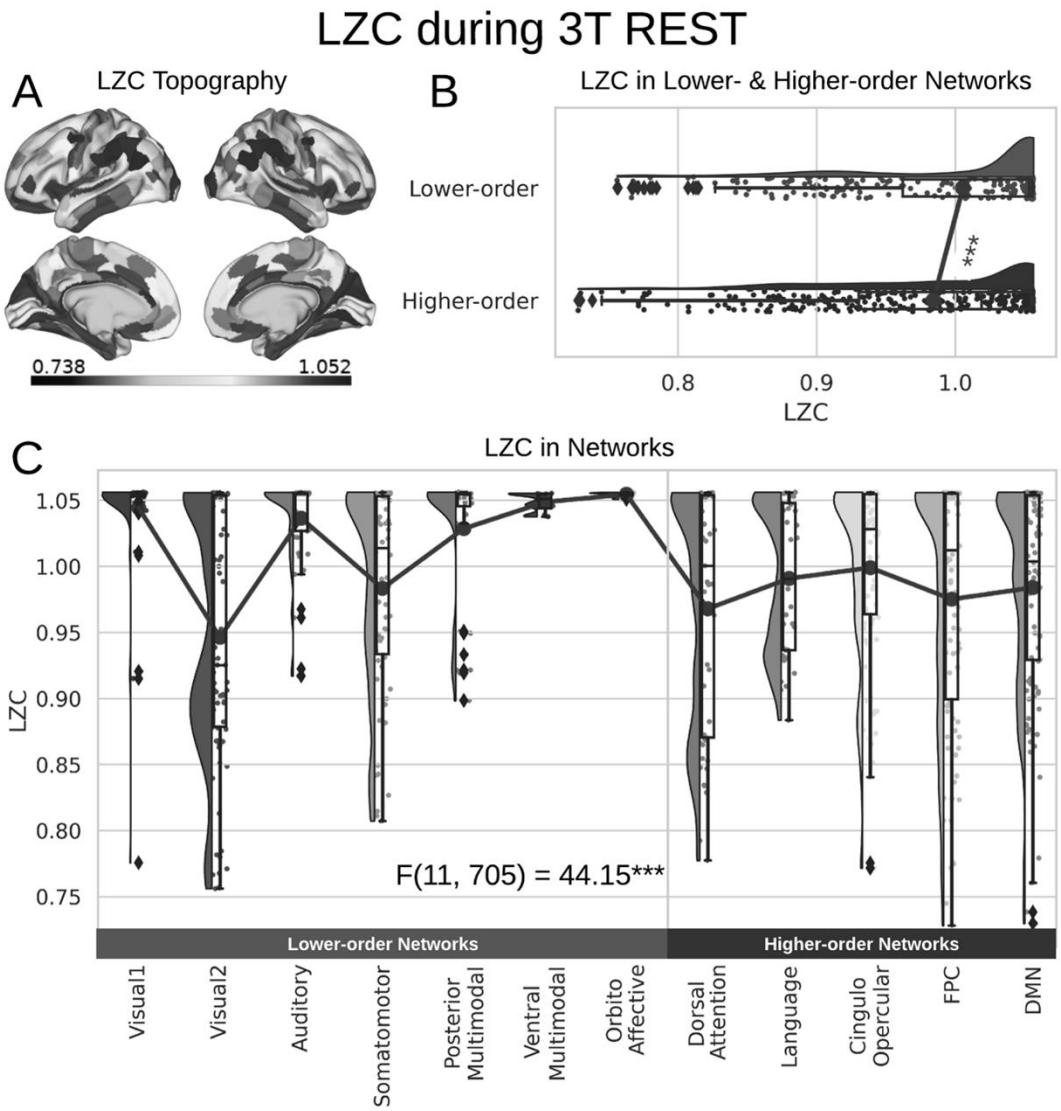

Supp. Fig. 1. LZC during the 3T resting state. Raincloud represent regions. **(A)** Spatial distribution of LZC during 3T REST condition. **(B)** LZC during rest for lower- and higher-order networks. Student's t-test showed significant ($p < 0.001$) differences between lower- and higher-order networks ($t = 3.60, d = 0.27$). This was also validated using Mann-Whiney non-parametric test ($U = 77278, \eta^2 = 0.03$) **(C)** LZC during REST for the 12 networks. One-way ANOVA showed a significant ($p < 0.001$) difference among the networks ($F(11, 705) = 44.15, \eta^2 = 0.40$) which was also validated using Kruskal-Wallis non-parametric test $H = 129.46, \eta^2 = 0.17$). Stars represent the significance level ($*** \equiv \alpha = 0.001$).

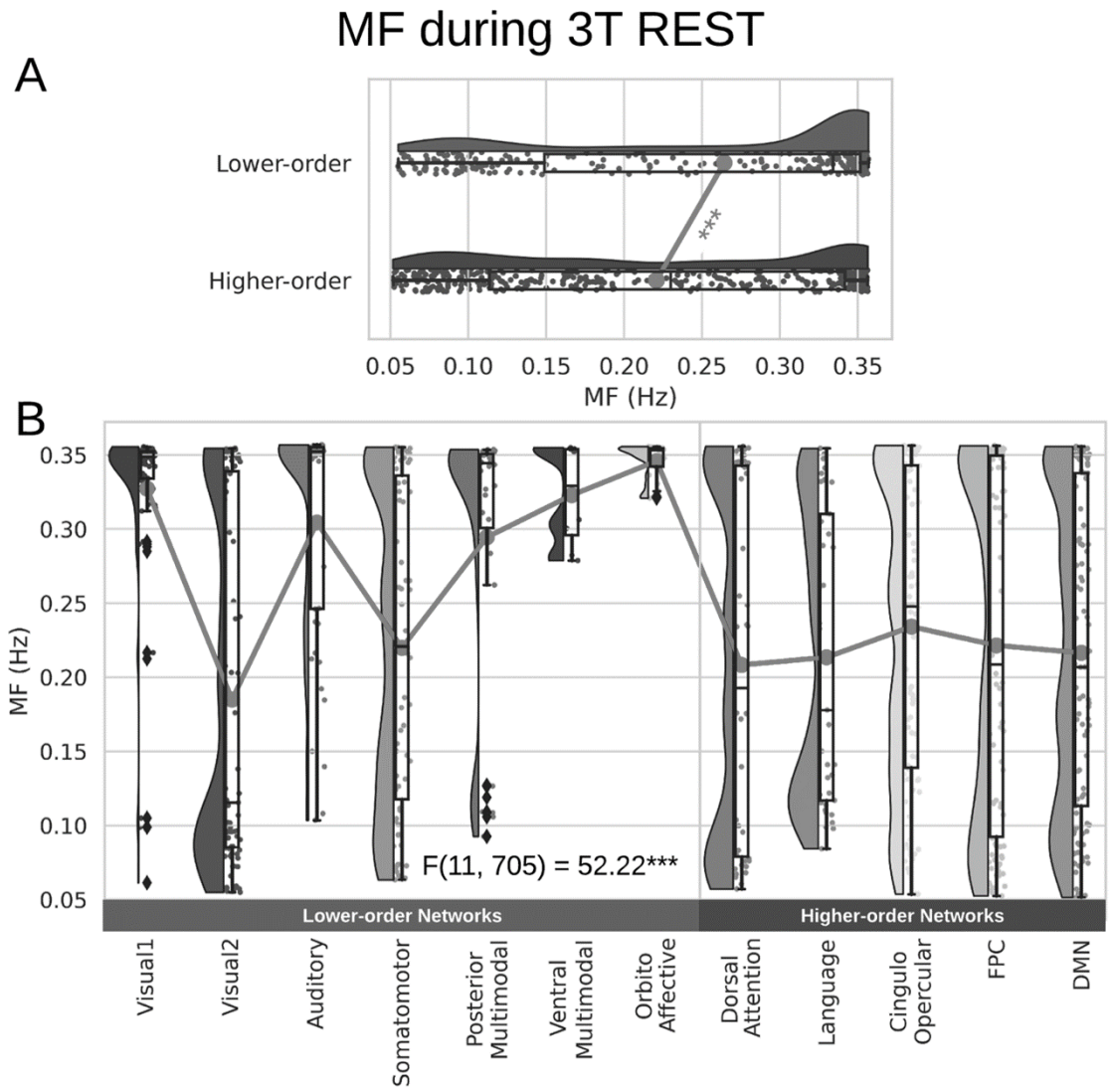

Supp. Fig. 2. MF during the 3T resting state. (A) MF during rest for lower- and higher-order networks showing higher MF in lower-order networks. **(B)** LZC during rest for the 12 networks. One-way ANOVA showed a significant difference among the networks.

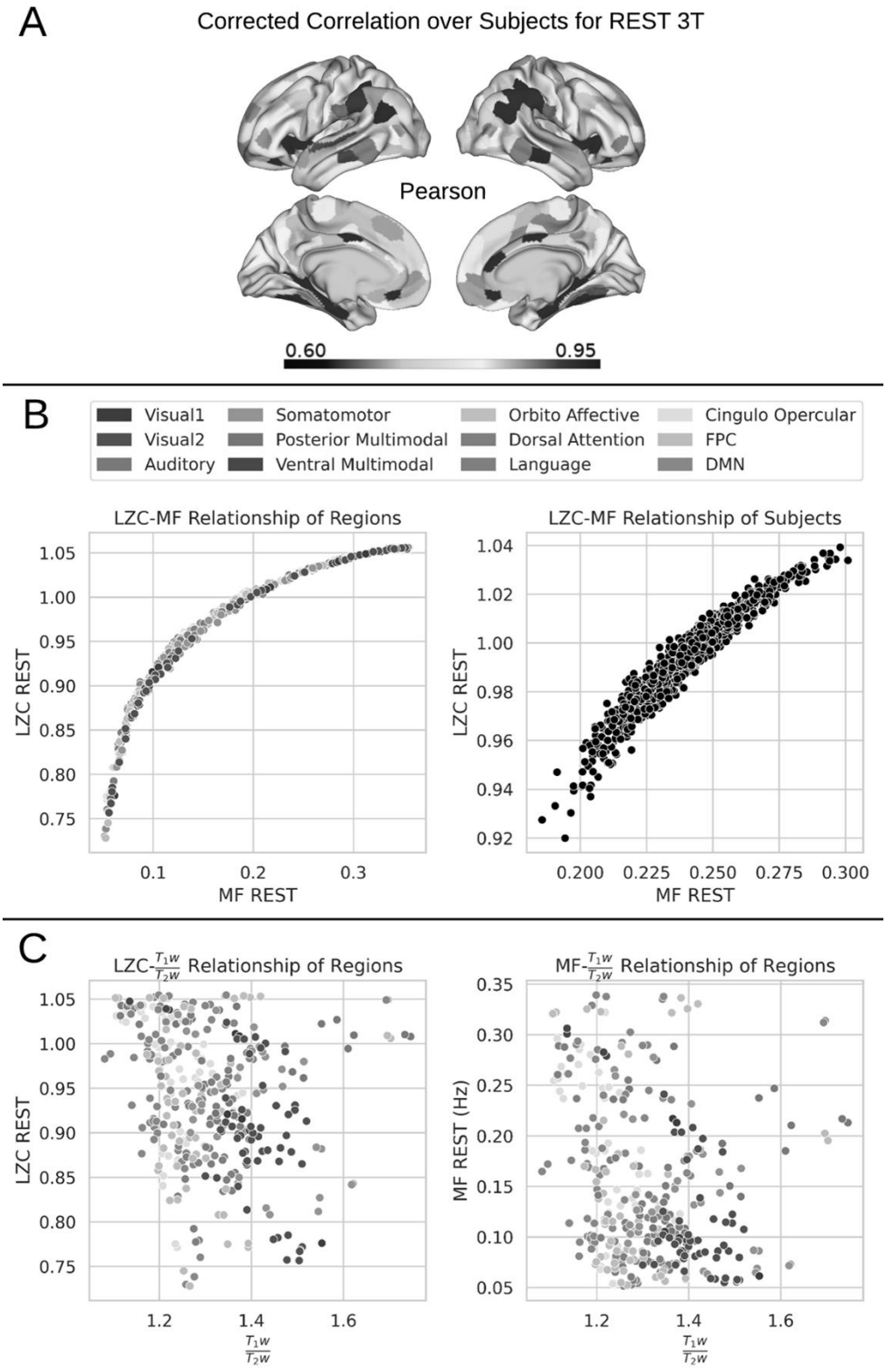

Supp. Fig. 3. The relationship between LZC and MF during 3T resting state. (A) Regional correlation between LZC and MF was computed by the Pearson method and corrected for multiple comparisons by the FDR method. **(B)** Regional scatter plots of LZC-MF relationship during 3T REST. LZC is plotted as a function of MF. Left shows scatter plot of regions averaged over subjects. Right shows subjects averaged over regions. **(C)** Scatter plots of LZC (left) and MF (right) as functions of structural T_1w/T_2w values. Each point is a region averaged over subjects.

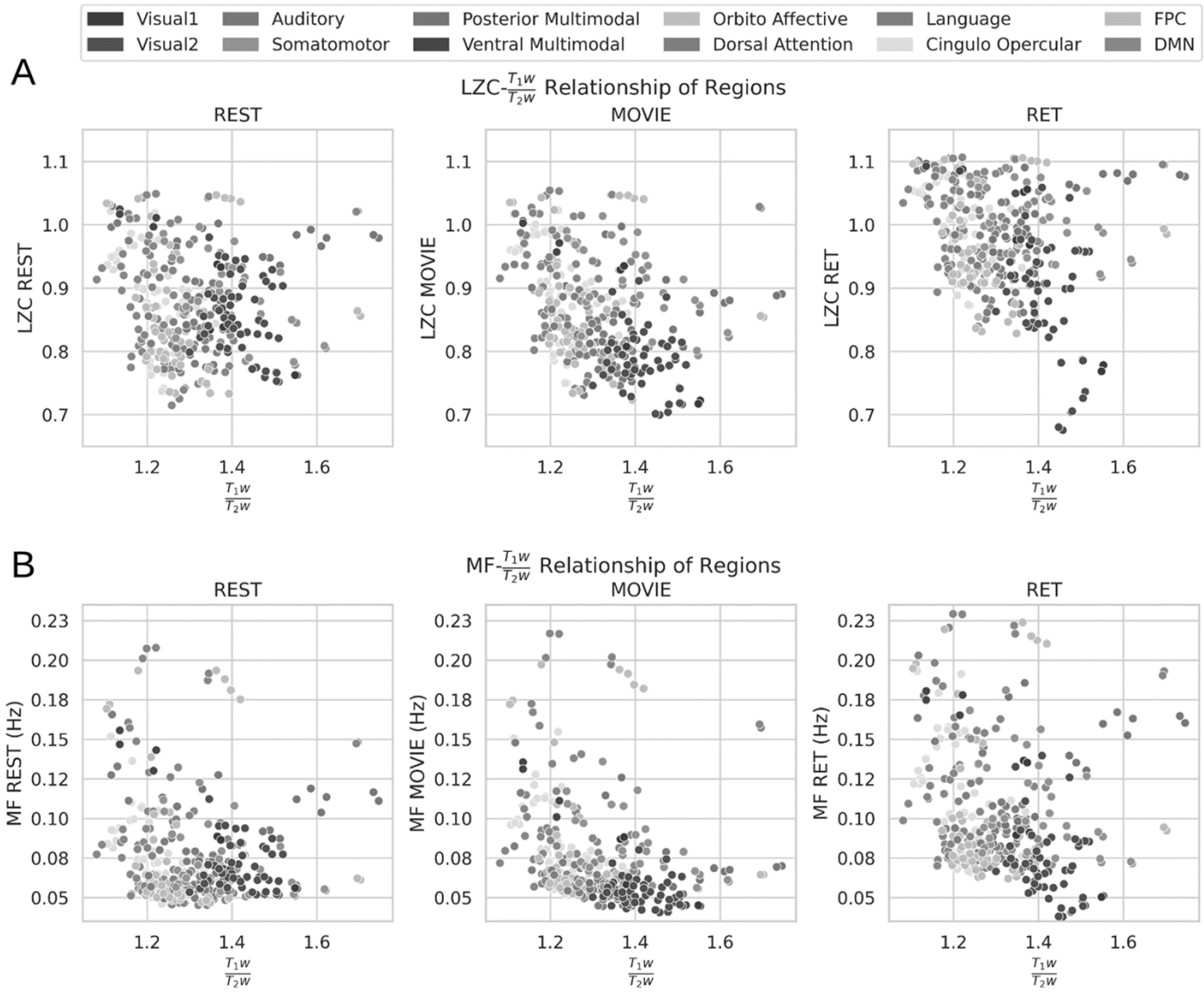

Supp. Fig. 4. LZC/MF relationship with T_1w/T_2w. The relationship between structural T_1w/T_2w values and LZC/MF. The distribution of LZC (A) and MF (B) values were calculated for each region and plotted as functions of their corresponding T_1w/T_2w values in all three conditions of REST (left), MOVIE (middle) and RET (right). No non-linear relationship can be observed.

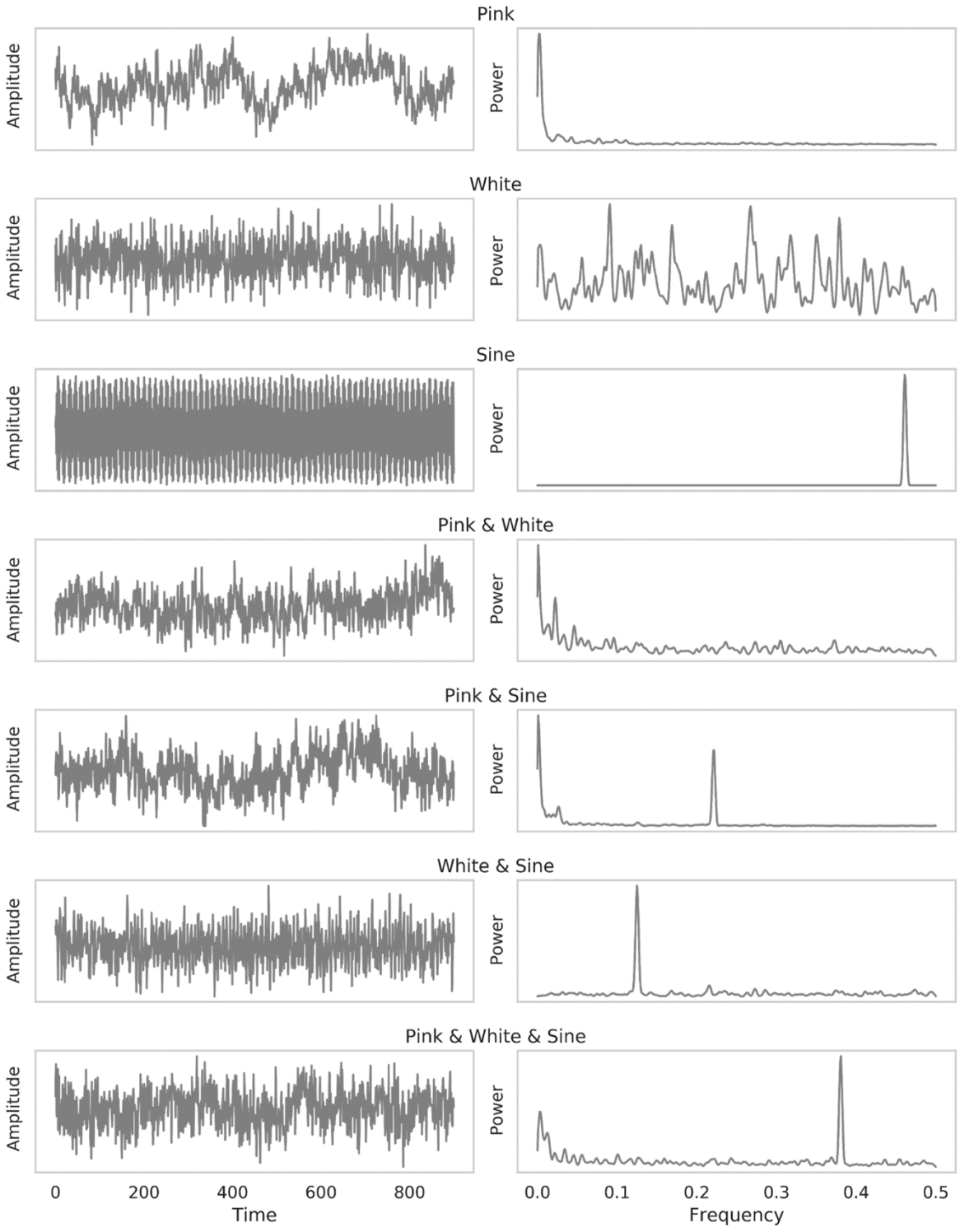

Supp. Fig. 5. Sample simulated signals in each category. Left plots are the sample signals in the time domain and the right ones are the same signals in the frequency domain (their power spectral distribution). For each category 5000 similar signals with different parameters were calculated and used in our LZC-MF relationship analysis.

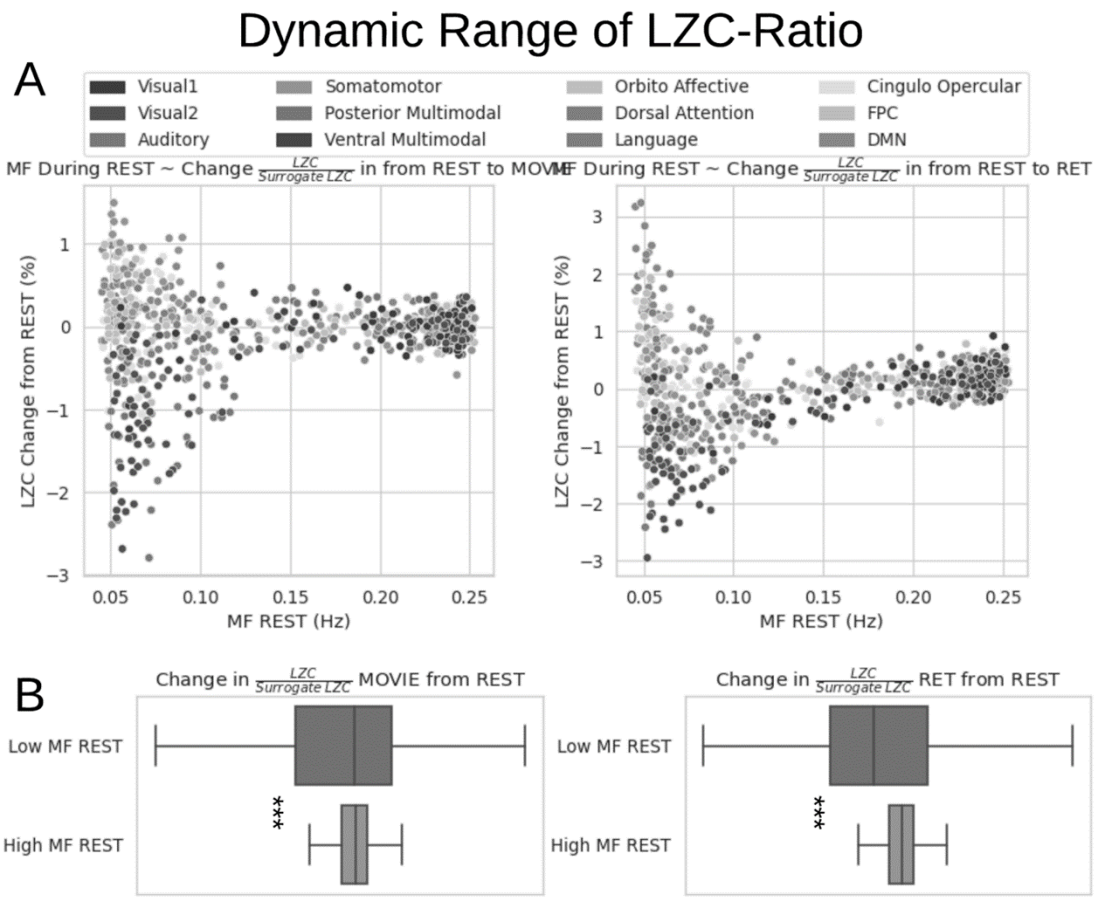

Supp. Fig. 6. The relationship between the change in LZC-Ratio from REST and MF during REST. The results for LZC-Ratio were similar to previous results for LZC (Figure 6) validating the dynamic range of LZC. Stars represent the significance level ($*** \equiv \alpha = 0.001$).

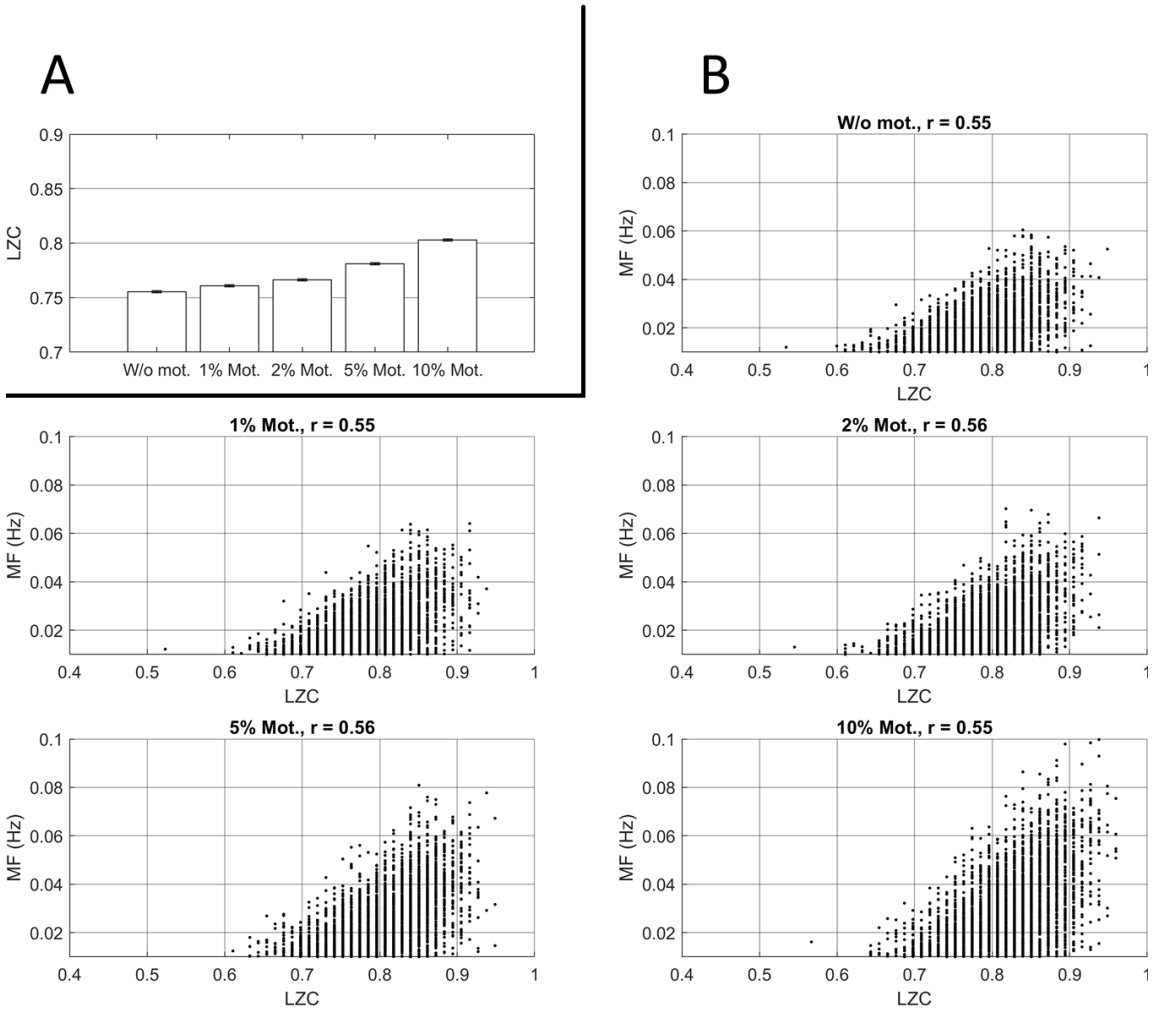

Supp. Fig. 7. Simulation of motion's effect. (A) Bar plot showing LZC values of 5000 pink noise signals without motion and with 1, 2, 5 and 10% of randomly chosen time points with motion simulated as an addition of a pseudorandom number between -4 and 4 to the amplitude of that time point. **(B)** Each scatterplot shows the LZC and MF values of simulated pink noises with and without motion, same as A. *R*-values are Spearman correlation coefficients between LZC and MF values.

References:

1. Hayes, A. F. Beyond Baron and Kenny: Statistical mediation analysis in the new millennium. *Commun. Monogr.* (2009) doi:10.1080/03637750903310360.
2. Tingley, D., Yamamoto, T., Hirose, K., Keele, L. & Imai, K. Mediation: R package for causal mediation analysis. *J. Stat. Softw.* (2014) doi:10.18637/jss.v059.i05.
3. Liu TT. 2016. Noise contributions to the fMRI signal: An overview. *Neuroimage*. 143:141–151.
4. Power JD, Mitra A, Laumann TO, Snyder AZ, Schlaggar BL, Petersen SE. 2014. Methods to detect, characterize, and remove motion artifact in resting state fMRI. *Neuroimage*. 84:320–341.
5. Jo HJ, Gotts SJ, Reynolds RC, Bandettini PA, Martin A, Cox RW, Saad ZS. 2013. Effective Preprocessing Procedures Virtually Eliminate Distance-Dependent Motion Artifacts in Resting State FMRI. Im C-H, editor. *J Appl Math*. 2013:935154.